

Bidirectional propagation of Action potentials

Jorin Diemer

Supervisor: Alfredo Gonzalez-Perez
Student Project
Niels Bohr Institute
University of Copenhagen
March 27, 2014

Acknowledgements

Firstly I want to thank Prof. Thomas Heimburg for giving me the opportunity to work in his group and for instructive conversations. Special thanks go to my supervisor Alfredo Gonzalez-Perez for taking a great deal of his time to give me a sufficient amount of knowledge and helped me in the lab as well as with the writing. Also I want to thank Alfredo for being patient and interesting talks about the topic as well as about non-scientific-related topics. Additionally I want to thank Tian Wang and Rima Budvyte, with whom I spent the most time in the lab.

Abstract

In this project we investigated bidirectional propagation of action potentials in giant axon of lobster *Homarus americanus*. We found an asymmetrical propagation in the giant axons from the first two walking legs, which have claws. The backpropagating antidromic action potential decreases the conduction velocity when we increase the stimulation voltage, while the forward propagating (orthodromic) action potential conduction velocity remains constant. The bidirectional propagation in giant axons from the third and fourth walking legs was found to be approximately symmetrical. Furthermore an analogy to backpropagation in dendrites was found.

Contents

Abstract	5
1 Introduction	9
1.1 The nervous system	9
1.2 Types of neurons	10
1.3 Glial cells	10
1.4 Action potential propagation	11
1.5 Backpropagation of Action potentials	12
1.6 Conduction velocity	13
1.7 Theories of nerve pulse propagation	13
1.7.1 The Hodgkin-Huxley theory	13
1.7.2 The soliton theory	15
1.7.3 Comparison of H-H and the soliton theory	16
2 Materials and methods	17
2.1 Sample preparation	17
2.2 Nerve sensory bundle extraction	18
2.3 Instrumentation	20
3 Results and discussion	23
4 Conclusion	39
A Appendix	41

Chapter 1

Introduction

1.1 The nervous system

The nervous system is responsible for sending and collecting informations through the body of both vertebrates and invertebrates, e.g. for pain detection or muscle contraction. It contains two classes of Cells, the nerve cells or "neurons" and the glial cells or "glia". They both have different functions to make the nervous system work.

We can classify neurons in three functional categories: sensory neurons, motor neurons and interneurons. While sensory neurons convey signals from the body's periphery to the nervous system, motor neurons communicate commands and decisions from the brain to muscles and glands. [9]

These neurons interact with each other via contacts called synapses. We have two main kinds of synaptic connections, an electronic, where a protein channel connects the cells or a chemical one. In a chemical connection the signal between two neurons is conveyed via neurotransmitters through the synaptic cleft. The network of these interactions of neurons is known as the nervous system. In the nervous system one distinguishes the central nervous system (CNS) and the peripheral nervous system (PNS). The aggregation of neuronal components organized in nerve cords along the midline of the animal is called CNS. The CNS contains dendrites and somata from motor neurons and all interneurons. In vertebrates the CNS runs along the back and is enclosed in bone, whereas in invertebrates the CNS runs along the abdominal side (see Fig.1.1).[10]

The CNS also contains the output branches of the sensory neurons. The PNS contains the sensory neurons and transmits signals from the periphery to the CNS, where the processing of the signal is done. The processing is located in regions with a density of interaction between neurons, consequently in regions with an high amount of synapses, the ganglia.[10]

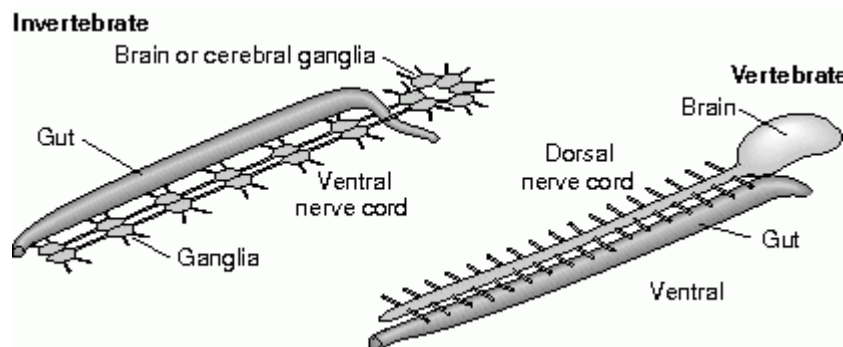


Figure 1.1: CNS of invertebrates and vertebrates [4]

1.2 Types of neurons

Neurons are the signaling units of the nervous system. They consist of a cell membrane, in which the cell organelles are embedded, like in other cells. Having several protrusions nerve cells differ in shape. Beside the cell body, called soma, the neuron has dendrites and an axon. The soma is the metabolic center of the cell, where all the organelles are located. While the dendrites are responsible for receiving incoming signals from other neurons, the axon carries the signal over distances from 0.1 mm to 2 m. The signals, called action potential, are inherently electrical and travel with a speed of 1 to 100 m/s. The action potentials are uniform in shape and therefore the information of a signal is determined by its pathway in the nervous system. One distinguishes between four groups of neurons: unipolar, bipolar, pseudo-unipolar and multipolar neurons (Figure 1.2).

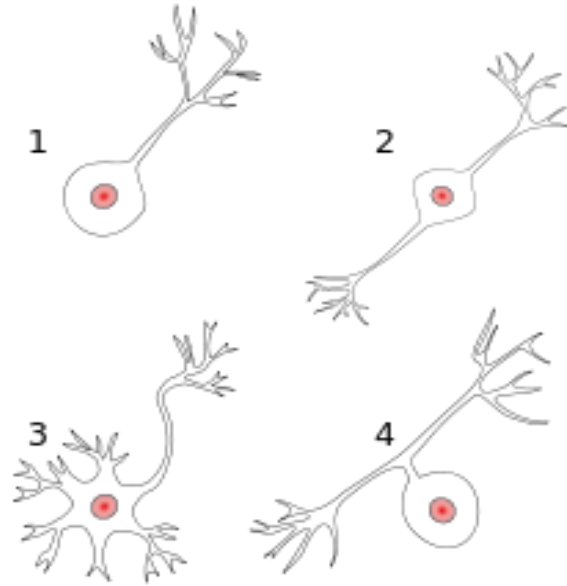


Figure 1.2: Types of neurons: 1) unipolar, 2) bipolar, 3) multipolar, 4) pseudo-unipolar [?]

Unipolar neurons have the simplest structure. They have one single branch, which splits into one branch serving as axon and several branches receiving signals, the dendrite. In a bipolar neuron has two separated branches originated in the soma. One dendritic structure receives the signals from the peripheric PNS and one axon conveying the signal to the CNS. Many sensory neurons are bipolar. In pseudo-unipolar neurons these two branches fuse close to the soma. Multipolar neurons possess many dendritic structures emerging from various points of the soma and an axon. Multipolar neurons generally act as motor neurons or interneurons. [9]

1.3 Glial cells

While neurons represent the active part of signal propagation, glial cells have a supporting role. In the nervous system exist four types of glial cells. Microglia and the macroglia astrocytes, oligodendrocytes and Schwann cells. Astrocytes the most present glia in the CNS. They supply neurons with needed nutrients, while connecting them with the blood vessels and acting as cellular "pipelines". Additionally Astrocytes prevent postsynaptic neurons from overexcitation, which could be deadly. Oligodendrocytes and Schwann cells insulate the axons by wrapping thin myelin layers around it. Oligodendrocytes are located in the CNS while Schwann cells support neurons the PNS. The insulation process is called myelination and allows sending signals very fast and over long distances. The myelin insulation has gaps, called Nodes of Ranvier. Microglia destroy invading microbes or leftovers of dead cells. In resting state microglia have

many branches, but after responding to invading microbes or dying cells the change in shape and start to travel to the origin of threat. They are the only motile glial cells and annihilate problems using phagocytose. [11]

1.4 Action potential propagation

Signal propagation can be described uniform for neurons, regardless of different neuron shapes and functions, in a model neuron. A signal travelling through the neuron can be seen as a linkage between four components. A input component, a trigger component, a long-distance component and a secretory output component. Each cell possess a resting membrane potential due to unequal distribution of ions. Ion pumps actively keep the K^+ concentration in the cell high and the Na^+ concentration low. The membrane is selectively permeable to K^+ ions due to porebuilding proteins called ion channels. Consequently K^+ ions diffuse down the ion gradient and lead to a negative charge inside the cell, consequently maintain the resting potential.

If it is possible to change the membrane potential rapidly, the cell is excitable, such as nerves and muscles. A reduction of the potential leads, dependent on a varying threshold, to an action potential due to changes in membrane permeability, such that the membrane is more permeable for Na^+ than K^+ [9]. This action potential travels through the axon, which connects the soma with the axon's terminal.

A signal can be induced by a physical stimulus (receptor Potential) or due to a registration of neurotransmitters (synaptic potential). This refers to the input component of the signal. These signals could lead to both depolarization and hyperpolarization. As mentioned depolarization could lead to an action potential, thus hyperpolarization has an inhibitory effect. Receptor and synaptic potential are graded, e.g. the amplitude and duration depends on the intensity of the physical signal respectively on the amount of neurotransmitter. The signals propagate passively and doesn't travel much farther than 2 mm. If an action potential is initiated, is verified in the trigger zone in the initial segment of the axon, more precise in the axon Hillock (figure 1.3) . This segment has the highest density of Na^+ channels, therefore the lowest treshold to generate an action potential, because a depolarization increases the percentage of open Na^+ channels. In the trigger zone all activities of synaptic and receptor potentials is summed up and the action potential is initiated, if the treshold is reached.

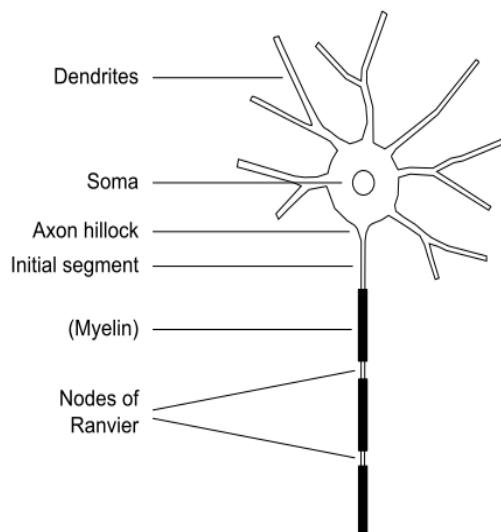


Figure 1.3: Schematic diagram of a neuron from reference [14]

The generated action potential is uniform in amplitude and shape, therefore the information is conveyed in the number of action potentials and their distribution in time. Once initiated the action potential travels without decay in amplitude along the axon until it reaches the neuronal terminal. There, each action potential leads to a release of neurotransmitter and the information is conveyed in the amount of neurotransmitter. After diffusion across the synaptic

cleft the transmitter leads to a synaptic potential in the postsynaptic neuron. This transmission is dependent on the type of receptor this potential is inhibitory (hyperpolarization) or exhibitory (depolarization).

1.5 Backpropagation of Action potentials

Talking about backpropagation one first has to remember the receptor and the synaptic potential, discussed in section 1.4. These potentials will in the following be called dendritic spikes, having their origin in the dendrites. Dendritic spikes occasionally pass the soma successfully and initiate an action potential. Both, the dendritic spike and the action potential can backpropagate in the dendrite and through the soma, respectively. Backpropagating signals diminish the chance of excitation in a time dependent manner and reduce the amplitude of following dendritic spikes. In case that the dendritic spike does not initiate an action potential, it backpropagates in its original dendrite (local backpropagation, Fig.1.4 A). If a dendritic spike successfully propagates through the soma and generates an action potential, this initiated action potential backpropagates through the soma and all dendrites, thus initiation of action potentials leads to global attenuation of dendritic spikes(Fig.1.4 B). [2]

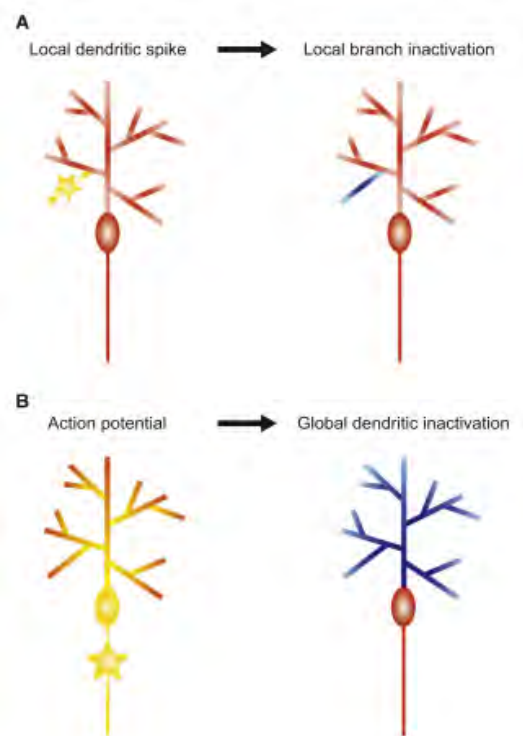


Figure 1.4: Local and Global Resets of Dendritic Excitability by Dendritic Spikes and Backpropagating Action Potentials. (A) Activation of a local dendritic spike that does not propagate effectively beyond its own branch reduces the ability of inputs to the same branch to trigger subsequent dendritic spikes. (B) When an action potential is triggered in the axon (either by a dendritic spike or by distributed input), its backpropagation into the dendritic tree causes a widespread reduction in the probability of dendritic spike generation. Figure obtained from reference [2]

Generally backpropagation controls the dendritic input. Waters et al. [16] determined the backpropagation after action potential generation in different neurons. They detected different intensity in the attenuation of the backpropagating signal. They normalized the dendritic spike to the somatic Action potential amplitude, so that they could compare the neuron's behaviour with increasing distance from the soma(Fig.1.5).

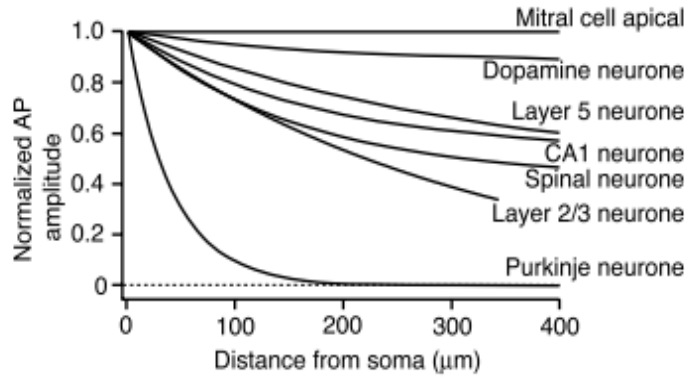


Figure 1.5: Dendritic Action Potential amplitude normalized to the somatic Action Potential amplitude and plotted as a function of the distance from the soma for different neurons. Figure obtained from reference [16]

In case of local backpropagation, the attenuation of dendritic spikes, which can be considered as a form of refractoriness or short-term plasticity can take almost 5 s to fully recover. The phenomenon of backpropagation can be exploited for computation and plasticity [2]. The time dependence of the spike attenuation and the differences in neuronal properties (Fig. 1.5) allow a various and diverse amount of signal processing. In this study I investigate if backpropagation is also possible, if the action potential is generated ectonic, i.e. not in the axon Hillock.

1.6 Conduction velocity

Two basic systems have been evolved for increasing nerve pulse velocities: Axonal giantism and Myelination. The axon can be represented by an equivalent circuit with the interior resistance (r_i), the transverse resistance (r_s) and the transverse capacity (c_s) (Fig. 1.6).

The conduction velocity increases, if the membrane can be charged faster. The charging is dependent of the longitudinal resistance ($r_i + r_o$) and the transverse capacity (c_m in Fig. 1.6A). The faster the charging, the smaller the product $(r_o + r_i) * c_m$ [6].

The interior resistance decrease quadratically with the axon diameter, therefore axonal giantism leads to faster conduction velocities. The myelination increase the transverse resistance (r_s in Fig. 1.6 B) and reduces the transverse capacitance (c_s).

The increase in transverse resistance increases the ratio of current along the axon to the current across the membrane, while the reduce in transverse capacitance decreases the amount of charge needed to generate a certain membrane potential. Due to less current across the membrane, the current in myelinated membranes is less attenuated over distance. This, additionally to the faster voltage change (due to decreases c_s), leads to an increase in action potential velocity. Anyway, increases in axon diameter and myelination increase the conduction velocity. [6]

1.7 Theories of nerve pulse propagation

In this section we will shortly introduce two different theories about nerve pulse propagation. The widely accepted Hodgkin-Huxley theory and the more recent soliton theory by Heimburg and Jackson [7].

1.7.1 The Hodgkin-Huxley theory

The Hodgkin-Huxley theory is based on ion current through voltage dependent ion channels. More precise the action potential is the result of a fast inward current of Na^+ and a more slowly activated outward current of K^+ . Additionally they assumed a leak current that consist mainly

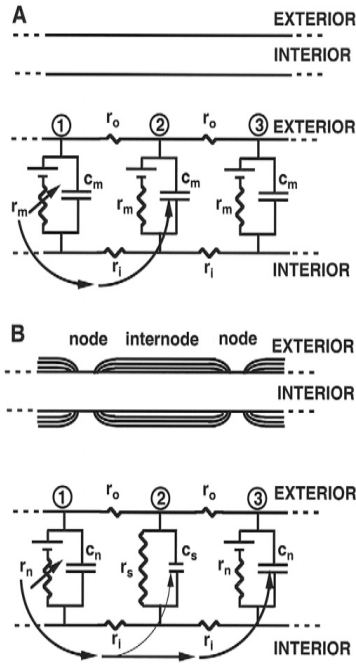


Figure 1.6: Axon as equivalent circuit. (A) non-myelinated (B) myelinated. Figure obtained from reference [6]

of Cl^- . The membrane potential is generated by different ion concentrations inside and outside of the cell. The channels can be represented as their conductances (Fig. 1.7).

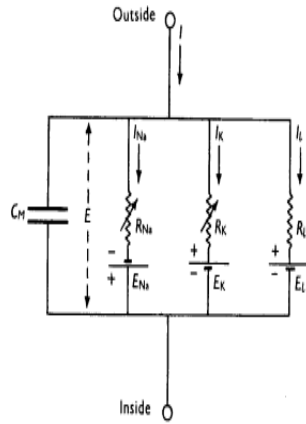


Figure 1.7: Equivalent circuit of H-H model. Figure obtained from reference [8].

While the leakage channel is voltage independent, the conductances g_{Na} and g_K represent the maximal channel conductances, correlating with an open state. The opening of the channels depends on gating particles, whose behaviour is not discussed here. The current through the membrane is described with

$$C \frac{du}{dt} = g_{Na} m^3 h (u - E_{Na}) + g_K n^4 (u - E_K) + g_L (u - E_L) + I(t)$$

The parameters m , h and n represent the probability of a gating particle to be in an open state. E_{Na} , E_K and E_L potentials generated by different ion concentrations inside and outside of the axon.

1.7.2 The soliton theory

The soliton theory treats the nerve pulse as a density wave propagating along the axon. Having its melting point slightly below body temperature, the membrane in resting state is fluid. During the nerve pulse it passes the transition point into a gel state. In transition heat capacity, lateral density and lateral compressibility changes in a non-linear manner, furthermore the lateral sound velocity depends on frequency (Fig. 1.8), this effect is called dispersion.

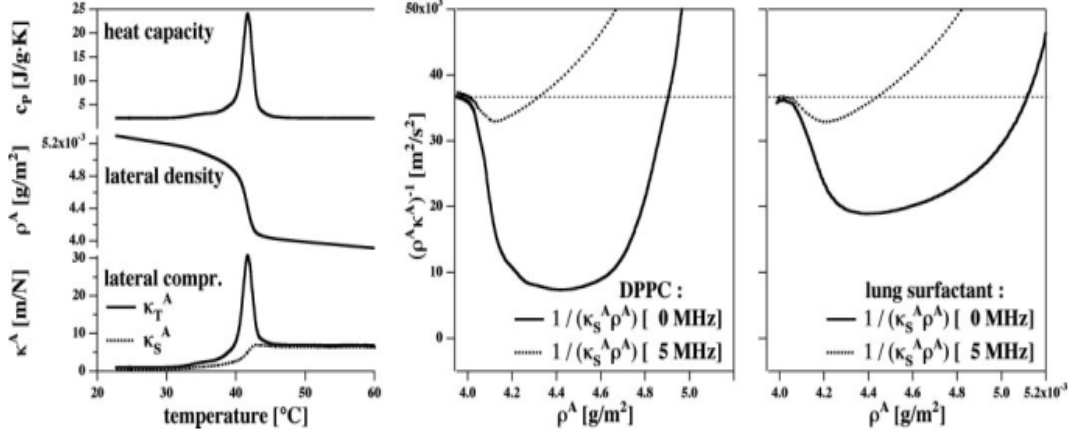


Figure 1.8: Behaviour of membrane properties in transition and frequency dependence of sound velocity. Figure is taken from reference [7].

The non-linearity and the dispersion are required for solitons. A solitary wave propagates with constant velocity and maintaining shape, therefore it is enabled to travel over long distances without a loss of energy. Mathematically a density wave with dispersion in one dimension is described by

$$\frac{\partial^2}{\partial t^2} \Delta \rho^A = \frac{\partial}{\partial x} \left[c^2 \frac{\partial}{\partial x} \Delta \rho^A \right] - h \frac{\partial^4}{\partial x^4} \Delta \rho^A$$

Where ρ^A is lateral membrane density, c is sound velocity in fluid phase of membrane, h is the linear parameter to set the linear scale of propagating pulse and the diminishing term represents dispersion.

Taking into account, that the sound velocity is frequency dependent one maintains, after coordinate transformation

$$\nu^2 \frac{\partial^2}{\partial z^2} \Delta \rho^A = \frac{\partial}{\partial z} \left[(c_0^2 + p \Delta \rho^A + q (\Delta \rho^A)^2 + \dots) \frac{\partial}{\partial z} \Delta \rho^A \right] - h \frac{\partial^4}{\partial z^4} \Delta \rho^A$$

Where ν is propagation velocity, p and q are the parameters determined from sound velocity and density dependence.

The voltage change during the nerve pulse is associated with changes in area and thickness of the membrane, which affect the capacitance. During the nerve pulse a reversible heat exchange is obtained and is proposed to be a result of lipid melting enthalpy. This heat flow is correlated with the voltage change and the density change during the pulse. Additionally the nerve pulse is adiabatic, because no energy is lost to the environment.

1.7.3 Comparison of H-H and the soliton theory

Appali et al.[1] listed the major differences of these two neural theories, which we show in the following paragraph.

Hodgkin-Huxley theory

H-H The action potential is due to the electric current conducted across the membrane by ion channels that act as resistors.

H-H Nerve pulse propagation is then explained as a moving self regenerating pulse of local capacitive discharges through the resistors followed by capacitor recharging.

H-H The theory is pure electrical with ionic hypothesis.

H-H The nerve signal or action potential is electrical pulse.

H-H The pulse propagation dissipates energy in the form of heat.

H-H The nerves physical changes are not explained.

Soliton theory

S The nerve pulse is a solitary wave generated by the lipid transition in the membrane.

S The propagation is due to the combined effect of non-linearity and dispersion.

S The theory is physical/ mechanical i.e. based on thermodynamics.

S The nerve signal is propagating adiabatic electromechanical pulse.

S The propagating pulse does not dissipate heat energy.

S The nerve changes dimensions and gets thicker during nerve pulse. The voltage pulse accompanies the propagating signal, as a result of these transient geometric changes of the membrane.

Both theories explain the electrical properties of a nerve pulse, but only in the Soliton mechanical changes and reversible heat exchange are predicted. [1]

Chapter 2

Materials and methods

2.1 Sample preparation

For the experiments nerve bundles from the walking legs of lobster *Homarus americanus* have been used. The lobster has four pairs of walking legs, which are different sized. The first and second legs have claws and are larger than the third and fourth legs (Fig.2.1).



Figure 2.1: Walking legs of lobster *Homarus americanus*. Blue line represents approximated progression of the nervebundles.

In the legs of a lobster, sensory neurons and motorneurons are gathered in three nerve bundles. A big, primary sensory bundle as well as a medium and a small bundle, which contain motor neurons. The soma is located in the ganglia of the thorax, while the axon stretch along the legs. In the big bundle giant axons with diameter of 65-150 μm are found. These giant axons are divided into two groups. One group contains 20-30 smaller giant axon with diameter between 65 μm and 80 μm and is located in the bundle's periphery. Another group, only present in the first and second legs, contains only five to six giant fibres with an diameter of 100-150 μm . These giant axons are located even more peripheric than the small giant axons. These giant axons are individually wrapped by thick (4-8 μm) layers. [15]. Besides the giant axons a large number of medium sized fibers with a diameter from 20 to 30 μm . The remaining processes consist of small axons, with an diameter less than 5 μm and organized in fascicles. [3] Figure 2.2 shows a corner of a nerve bundle. A nerve bundle contains hundreds of axons grouped together in sheat encased fascicles. Consequently there exist three extracellular compartments.

The space between the axons inside the fascicles is called peri-axonal (PA). The room between the fascicles is called peri-fascicular (PF) and the outside of the bundle is the solution bath. [?]

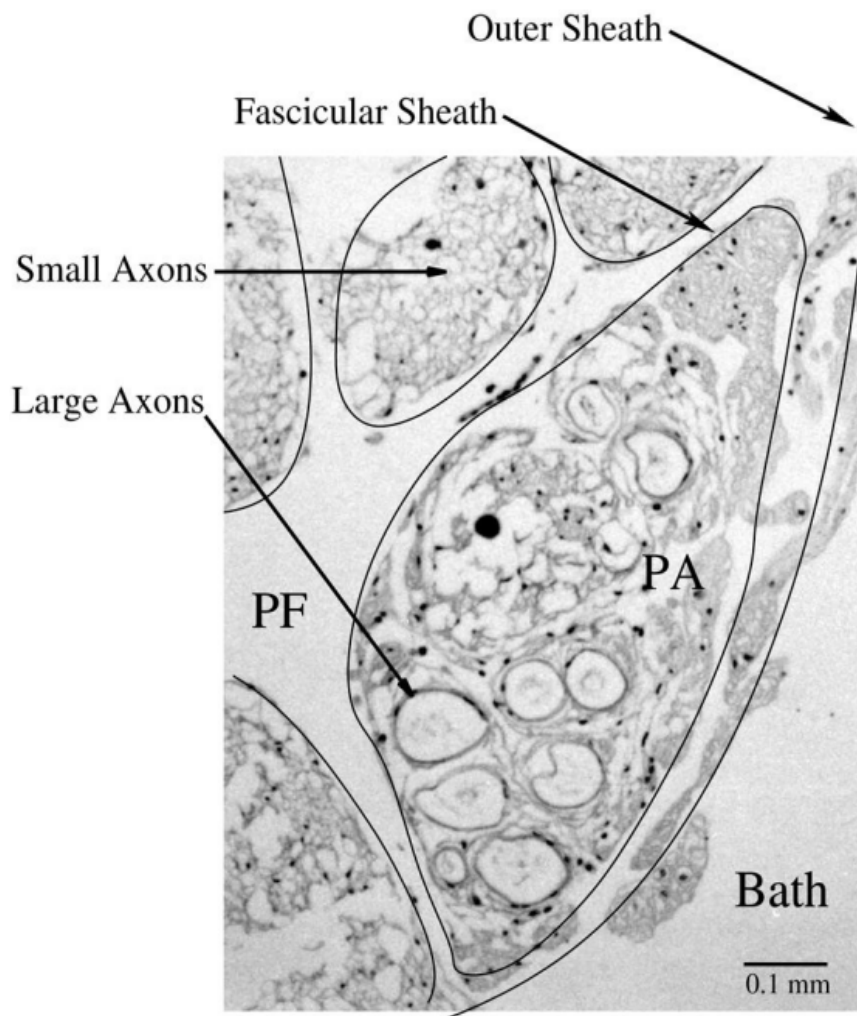


Figure 2.2: Axon distribution in a nerve bundle of a lobster nerve. Fascicular and outer sheath are highlighted and the three extracellular compartments are shown (PA, PF and Bath). The Giant Axons are located in the bundles periphery as suggested. Figure obtained from reference [5]

2.2 Nerve sensory bundle extraction

The lobster *Humarus americanus* was bought from a local fish dealer (Fiskerikajen, Frederiksborggade 21, 1360 København). Over night it was stored in a fridge. First the legs were chopped at the Ischiopodite. The legs could be stored for two days in cooled solution, without a loss in nerve activity. The used solution was composed of: 465 mM NaCl, 2 mM KCl, 25 mM CaCl₂, 8 mM MgCl₂, 4 mM K₂SO₄ and 3 mM Glucose in 1 l of distilled water. The pH was adjusted to 7,4 with NaOH.

The entire dissection process was performed in solution. The carapace was cutted with a scissor on both sides of the leg from the Ischiopodite to the Carpopodite (Fig.2.3), so that the upper carapace could be gently removed, by carefully lifting the cutted carapace with a

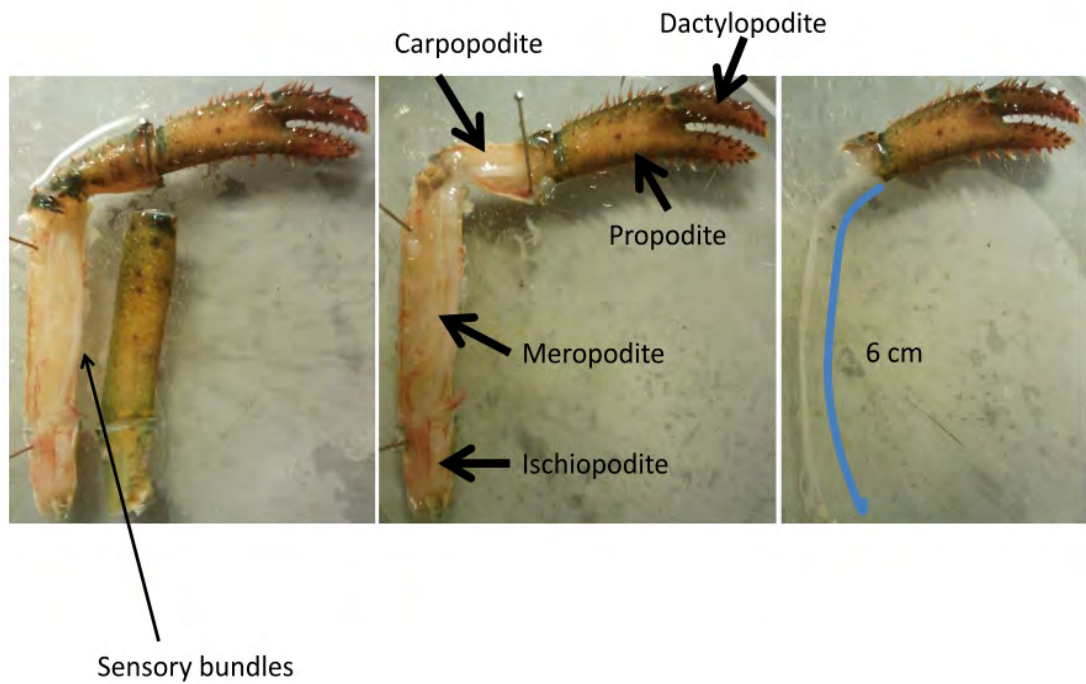


Figure 2.3: This Figure shows steps of the dissection as well as the anatomical parts of the lobster walking leg. Left: Clearly visible big bundle after removing first part of the carapace. Middle: The upper carapace of the Carpopodite was also removed and the bundle could be pulled out of the nerve and be cut between Carpopodite and Propodite. Right: Here the big bundle's connection to the Propodite was preserved, the rest of the Carapace was removed and the approximate length sketched.

tweezer while cutting connections of muscles to it with a scalpel. Following the carapace of the Carpopodite was removed in the same way. During the process the leg was fixed with pins, to avoid movement. After the successful removing of the upper carapace the large and medium bundles were clearly visible. With small, vitreous sticks the bundles were pulled out of the leg into the solution, starting at the Ischiopodite. In the end the bundle was chopped at between Carpopodite and Propodite. The extracted bundles were transferred to petri dish with the saline solution (Fig.2.4).

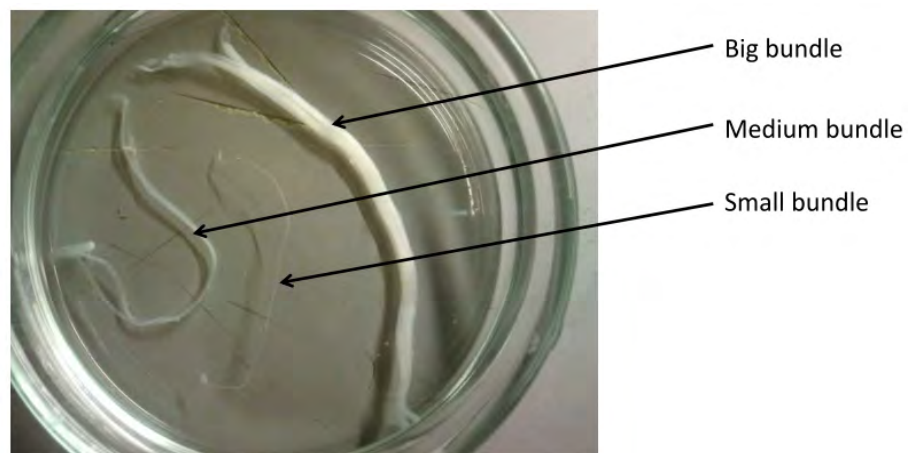


Figure 2.4: Bundles from a lobster walking leg after dissection in solution.

To run the experiment the big bundle was transferred to a nerve chamber (next section) as soon as possible.

2.3 Instrumentation

The nerve chamber as used in the experiment is shown in figure 2.5. The chamber consists of plexiglass, wherein pins were fixed. The nerve bundle was placed on the pins and was stimulated from outside of the bundle (external stimulation). The distance between two pins was 0,25 cm, therefore the used nerve chamber had a pin array of 5,25 cm. The diameter of a pin was 0,6 mm, made of stainless. At the ends of the chamber were pockets filled with solution to prevent the bundle from drying. The chamber was covered with a glass lid to avoid drying.

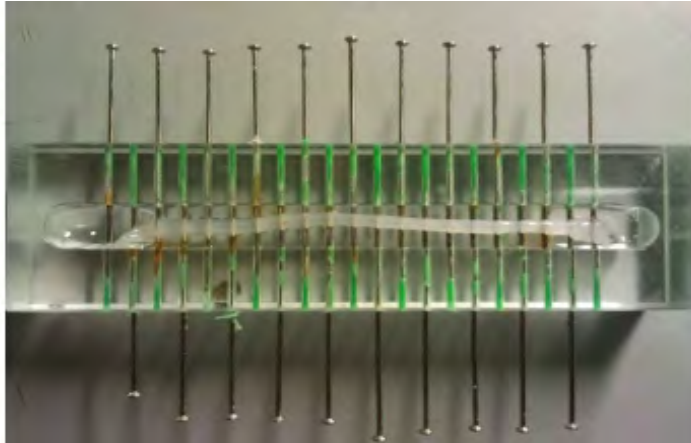


Figure 2.5: Nerve chamber with large bundle. The bundle has its ends in the solution chambers.

For recording and stimulation we used a PowerLab 26T from AD instruments, as in shown in figure 2.6, with an integrated Bio-amplifier. Further information can be found on the company webpage [13]. This instrument is able to record with two channels at a time.



Figure 2.6: PowerLab 26T. In the left the output connection, used for the generation of the stimulation signal, while in the right the Bio-amplifier is connected to the recording channels.

To measure the bidirectional propagation the bundle was excited through the stimulation

channel. On both sides of the stimulation a recording channel was positioned. Each channel, the stimulation channel as well as the recording channel has an anode and a cathode. Additionally an earth was placed between the stimulation channel and the recording channels, respectively. The anode of the recording channels had to be closer to the stimulation as the cathode to get an uninverted signal. One possible configuration is shown in figure 2.7. Figure 2.8 shows a sketch of the experimental setting.

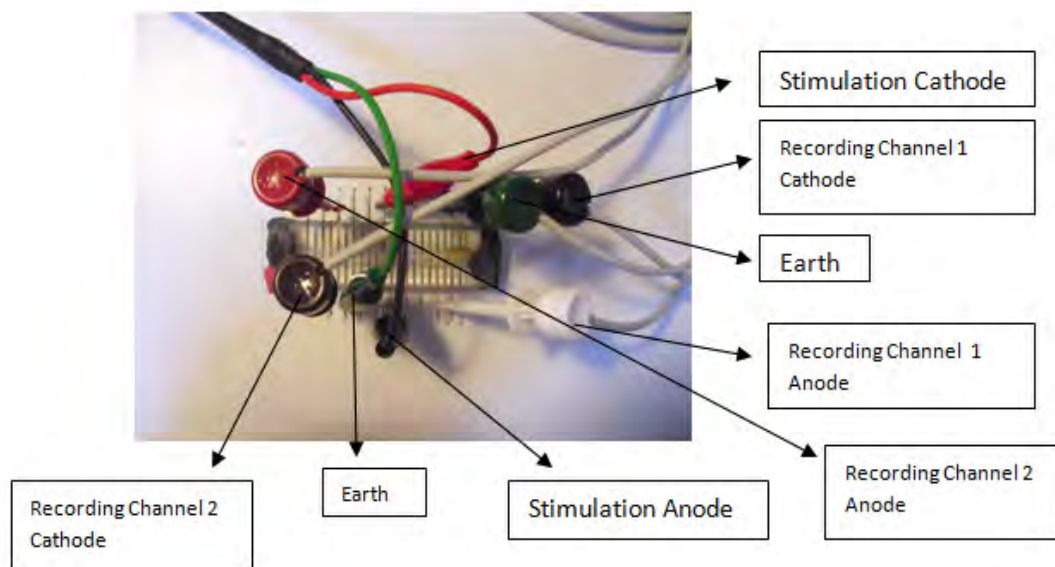


Figure 2.7: Likely electrode configuration during a measurement.

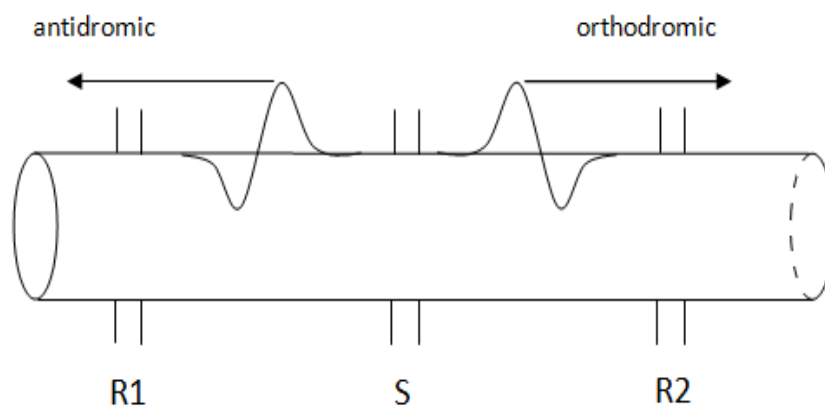


Figure 2.8: Sketched experimental setting. R1 and R2 are recording channels, while S refers to the stimulation. Propagation of action potentials in antidromic and orthodromic direction.

The signal was processed with the software LabChart7pro. It images the stimulation channel and the recording channels as in figure 2.9. The distance between the channels was calculated out of the number of pins between the anode of the recording channels and the next electrode of the stimulation channel. The stimulation took place after a time of 0,003 s. The first peaks in the recording channels refer to a stimulation artefact and not to an action potential. This stimulus-artefact could be minimized by placing the earths as close as possible to the recording channels. The second peaks refer to an action potential measured in the

bundle. The nerve bundle was placed with its ends in the solution. With this setup it was possible to easily change distance and position from all channels, therefore it was simple to find configurations with a clear signal as shown in figure 2.9.

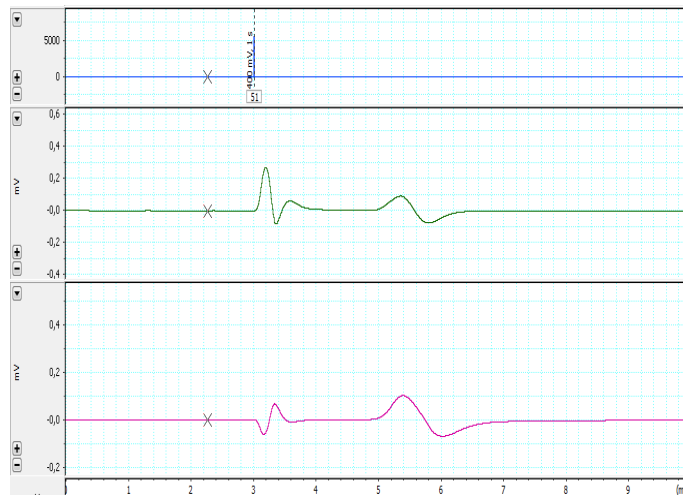


Figure 2.9: LabChart data 19.3.02

Blue: Stimulation Channel, Green: First Recording Channel, Red: Second Recording Channel

The data were exported from Labchart7pro in a text file and imported to OriginPro 9.1. From the location of a peak we determined the propagation velocity of an action potential, by dividing the distance between stimulation and recording channel by the calculated time from stimulation to the first peak of the action potential signal. Note that the "stimulation" ("stimulus") artefact can change in intensity (height) depending on their proximity to the recording electrodes as well as the position of the ground. Because the ground of the stimulation cables have to be in one of the propagating sides generally the stimulus artefact appearing for the antidromic and orthodromic signals are different.

Chapter 3

Results and discussion

It is generally known that the action potential (AP) is generated in the axon Hillock (Fig. 1.3) and propagates away from the soma to the neuron's terminus or synaptic area. Nevertheless, backpropagation of APs through the soma into the dendrites was observed [16] [14] [12]. Backpropagation is believed to be important for neuronal signal control, hence for neuronal function and plays a key role in synaptic plasticity and neuronal computation [2]. It is generally known, that an AP can be artificially generated in ectopic sites of a neuron. We intend to investigate the bidirectional propagation of Action potentials in giant axons in order to explore possible asymmetries in the AP propagation, as a function of the stimulation Voltage. As a experimental model we chose the large sensory bundle of the walking legs from a lobster, since it contains a limited number of giant axons. The preparation and execution of the experiment was performed as described in "Materials and Methods".

As a first step we had to identify the generation of the APs, corresponding in the giant axons. We assorted the walking legs in two categories. The first and second walking legs have claws and build the first category (Category "Claw"). The second category represents third and fourth walking legs, since they don't have a claw (Category "NoClaw"). The grouping was performed, since differences in neuronal arrangements are present in both groups. In figures we show 3.1 to 3.4 we show the results of measurements with one bundle of each category. They show AP propagation in orthodromic and antidromic direction for different stimulation Voltages, respectively. Figures 3.1 and 3.2 correspond to the measurement 19.1.01. Since every measurement took place in february 2014 the "19" defines the date of it. The single "1" means, that it was the first bundle used on this day and "01" signifies, that it was the first measurement, which was done with the bundle. Figures 3.3 and 3.4 correspond to measurement 14.1.01.

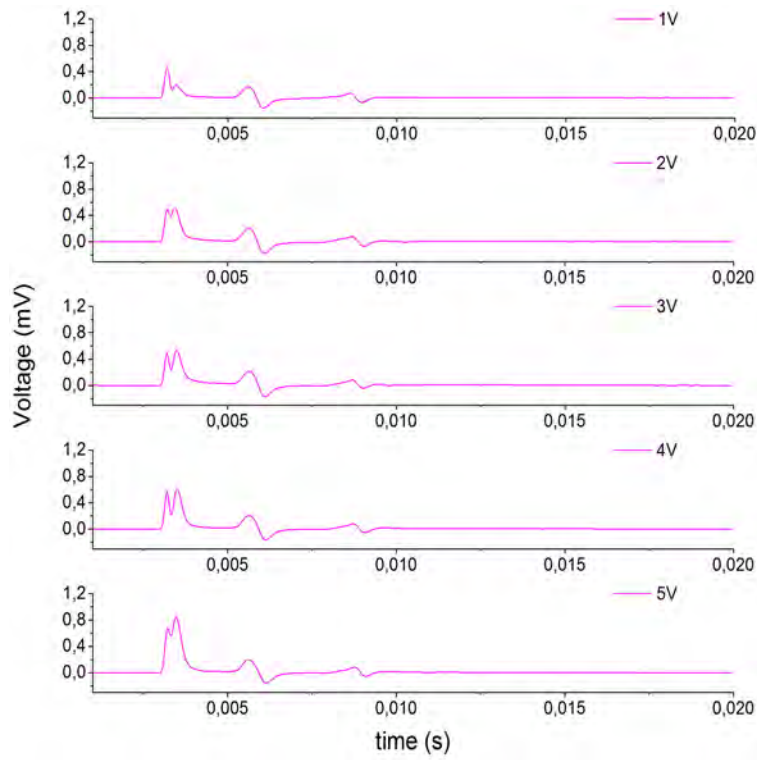


Figure 3.1: Orthodromic AP propagation for bundle 19.1.01 from category "Claw". Amplitude for stimulation Voltages from 1V to 5V.

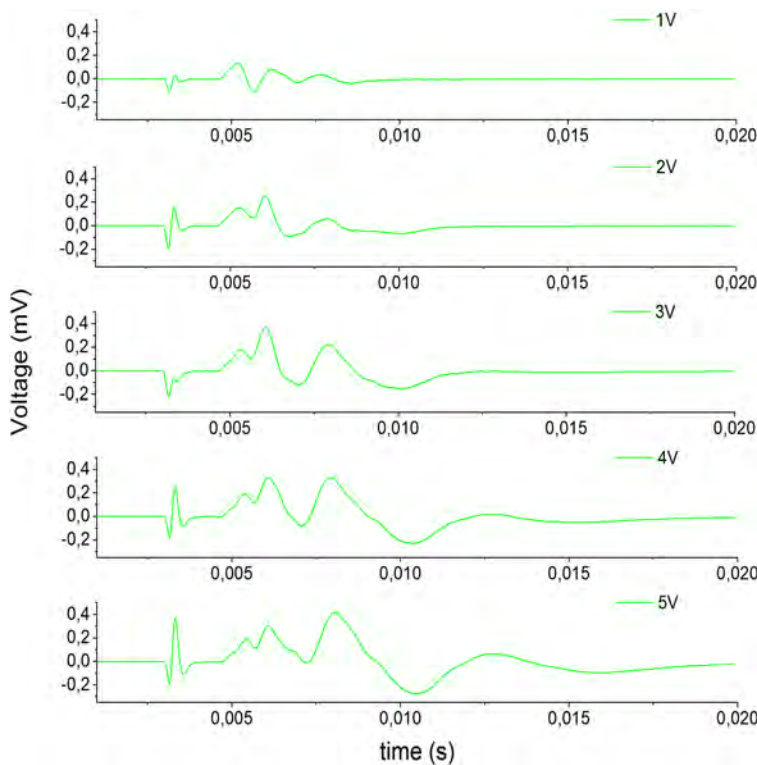


Figure 3.2: Antidromic AP propagation for bundle 19.1.01 from category "Claw". Amplitude for stimulation Voltages from 1V to 5V.

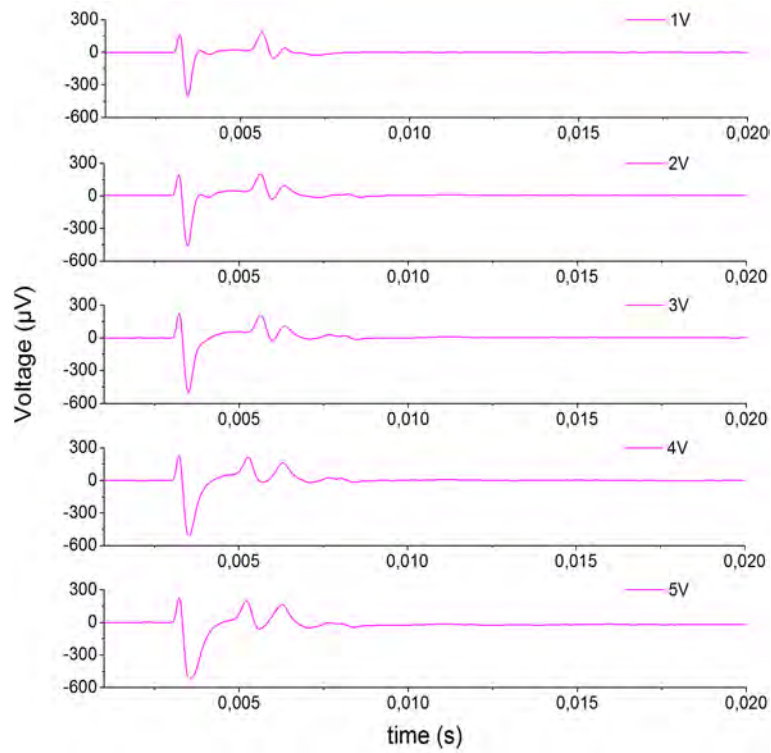


Figure 3.3: Orthodromic AP propagation for bundle 14.1.01 from category "NoClaw". Amplitude for stimulation Voltages from 1V to 5V.

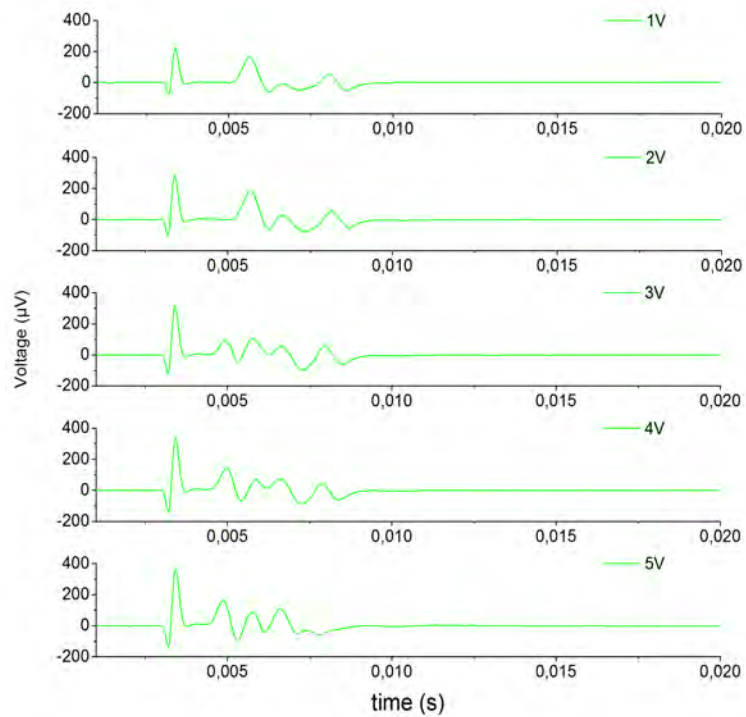


Figure 3.4: Antidromic AP propagation for bundle 14.1.01 from category "NoClaw". Amplitude for stimulation Voltages from 1V to 5V.

The number of peaks depends on the polydispersity of the axonal diameter, since several axons with identical diameter would lead to one peak. Axons with a larger diameter lead to an earlier peak in the spike histogram, since APs propagate faster with larger diameter[6]. This varies depending on the preparation (animal).

In attempt to compare the results of different measurements, we had to be sure, that all giant neurons were excited. So that the peaks, which correspond to similar axons are comparable. The stimulation voltage was delivered for a duration of 0,05 ms and the intensity was increased in steps of $\leq 0,2V$. At lower stimulation voltages not all giant neurons are excited, so that the number of peaks varies. After reaching a treshold the number of peaks stays constant (Fig. 3.5 - Fig. 3.8). However, the shape and position of the peaks can change also at stimulation voltages higher than the treshold. It was found that at stimulation voltages about 2V all neurons were excited and consequently the number of peaks didn't change at higher stimulation voltages.

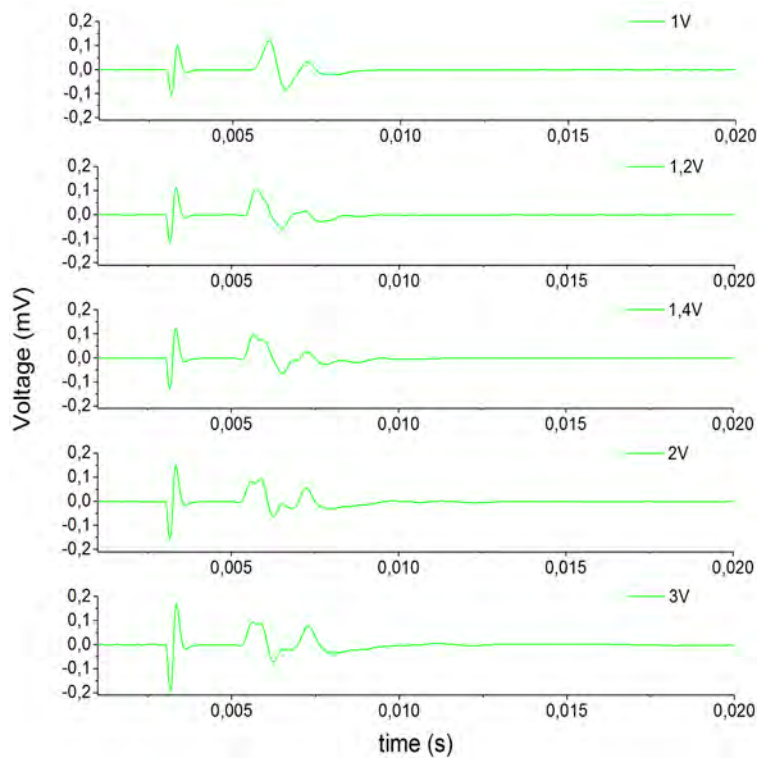


Figure 3.5: Antidromic AP propagation for the bundle 19.3.01 from category "Claw" at different stimulation voltages. Number of peaks after stimulation with 2 V and 3 V constant, while it varies between 1 V , 1.2 V and 1.4 V, respectively.

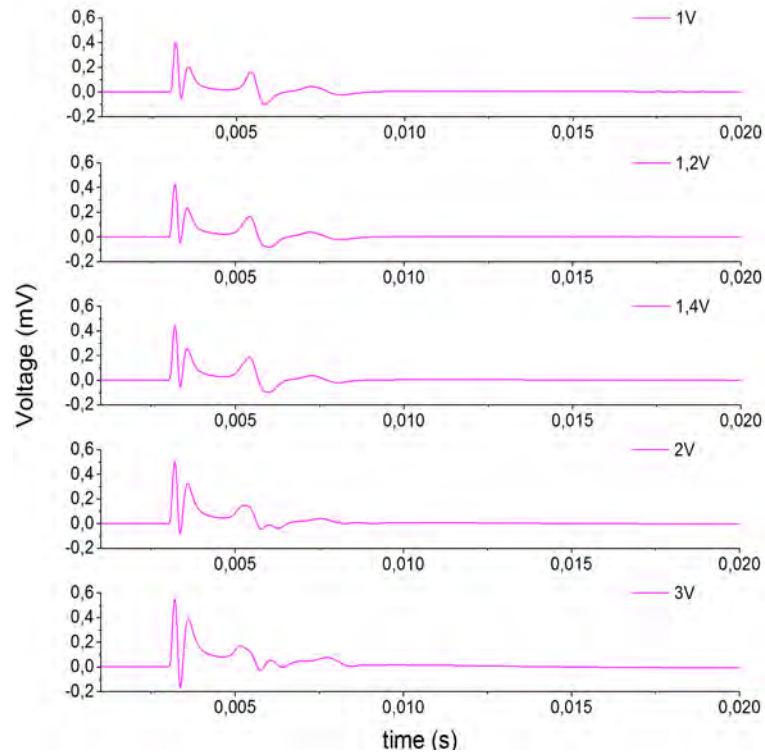


Figure 3.6: Orthodromic AP propagation for the bundle 19.3.01 from category "Claw" at different stimulation voltages. Number of peaks after stimulation with 2 V and 3 V constant, while it varies between 1.4 V and 2 V.

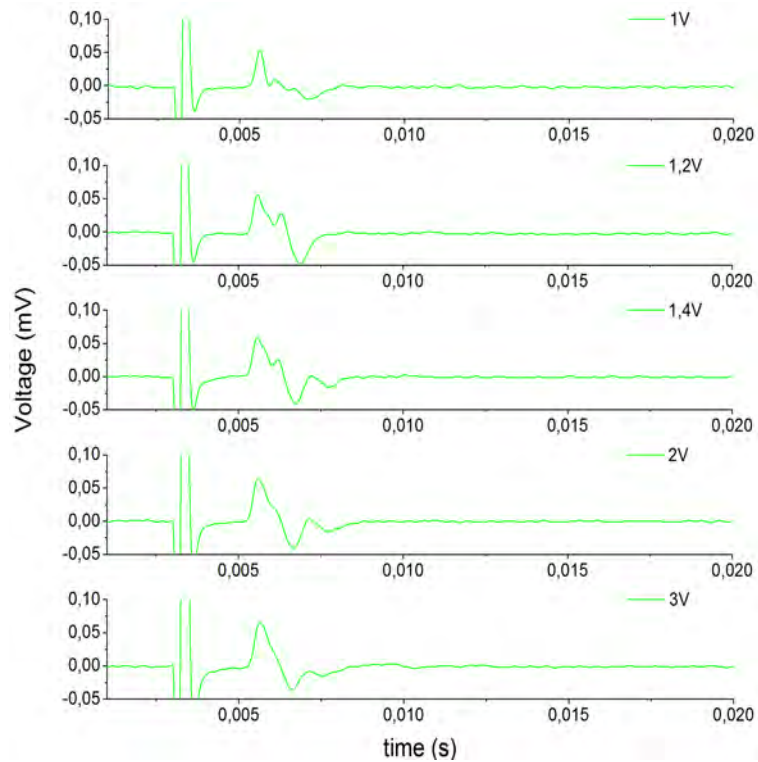


Figure 3.7: Antidromic AP propagation for the bundle 20.2.01 from category "NoClaw" at different stimulation voltages. Number of peaks after stimulation with 2 V and 3 V constant, while it varies between 1 V , 1.2 V and 1.4 V, respectively.

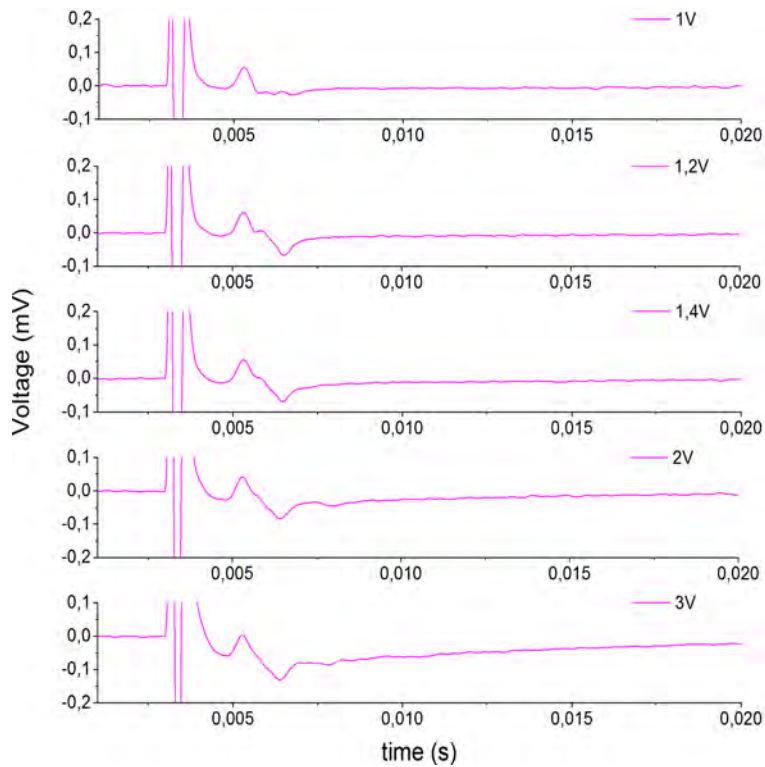


Figure 3.8: Orthodromic AP propagation for the bundle 20.2.01 from category "NoClaw" at different stimulation voltages. Number of peaks after stimulation with 2 V and 3 V constant, while it varies between 1 V and 1.2 V.

Due to these observations a stimulation voltage of 2V had been chosen as the threshold, at which all neurons in a bundle are excited ($V_t = 2V$). More reasons for the chosen threshold will be presented later. However, in some rare cases even at stimulation voltages above the threshold, the number of peaks changed (e.g. Fig. 3.4). These cases haven't been regarded in calculations. An explanation for that behaviour could be, that the stimulation took place on the outside of the bundle, so that the distance to the neurons was not uniform. It is well known, that the distance between the stimulation electrode and the neuron influences the threshold voltage necessary to generate an AP (Figure 3.9).

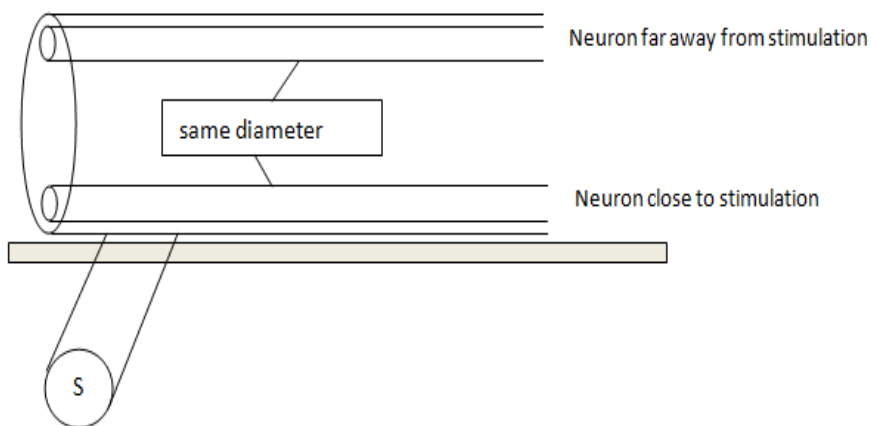


Figure 3.9: The neuron close to the stimulation needs less voltage to be excited, if the neurons have the same diameter. S represents the stimulation site

The giant axons are located in the periphery of the bundle (Figure 2.2), what makes it difficult to always get the spikes correlated with the diameter to stimulation voltage. In neurons with larger diameter the AP propagates with higher velocity and generally the neurons are excited at lower voltages. We took the first and second peaks as correspondence to the giant axons, because they are the fastest axon present in the bundle.

After we performed all the experiments at different stimulation voltages we had to calculate different parameters associated with the APs for the first and second peak, corresponding to the giant axons. We determined the propagation velocity, the intensity and the width of each AP. The velocity was calculated by taking the time from stimulation to the peak of the AP and the distance to the recording channel. The intensity was estimated by the peak-to-peak distance and the width by the extension of the AP. Figures 3.10 and 3.11 show examples of AP velocities in giant axons for the two categories of legs, respectively.

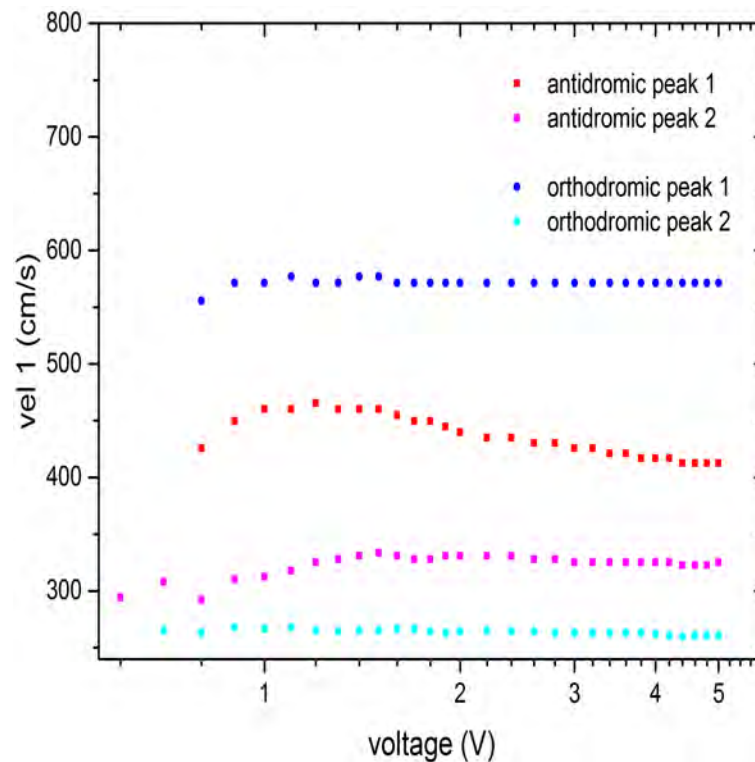


Figure 3.10: AP velocities from 19.1.01 ("Claw"), corresponding to giant axons in orthodromic and antidromic direction.

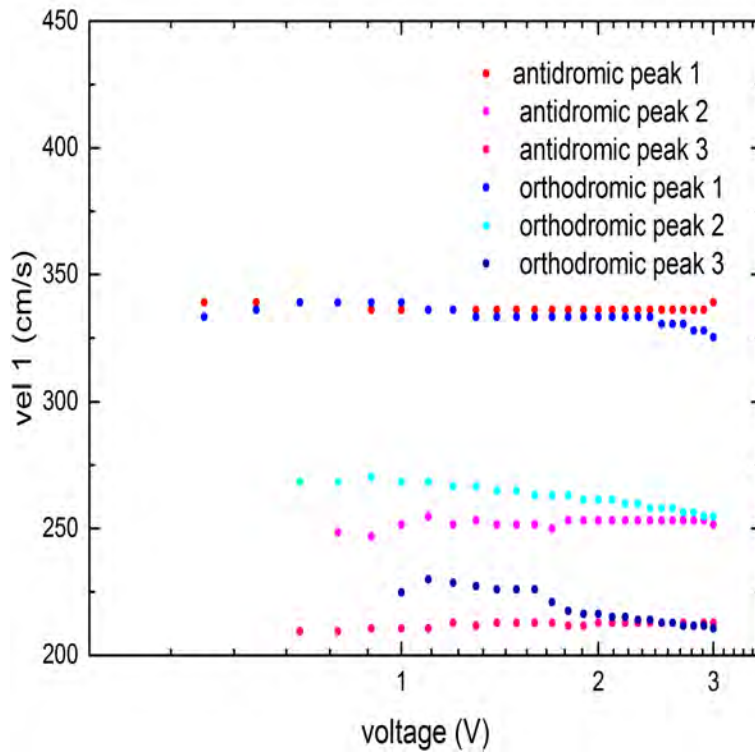


Figure 3.11: AP velocities from 14.1.05("NoClaw"), corresponding to giant axons in orthodromic and antidromic direction.

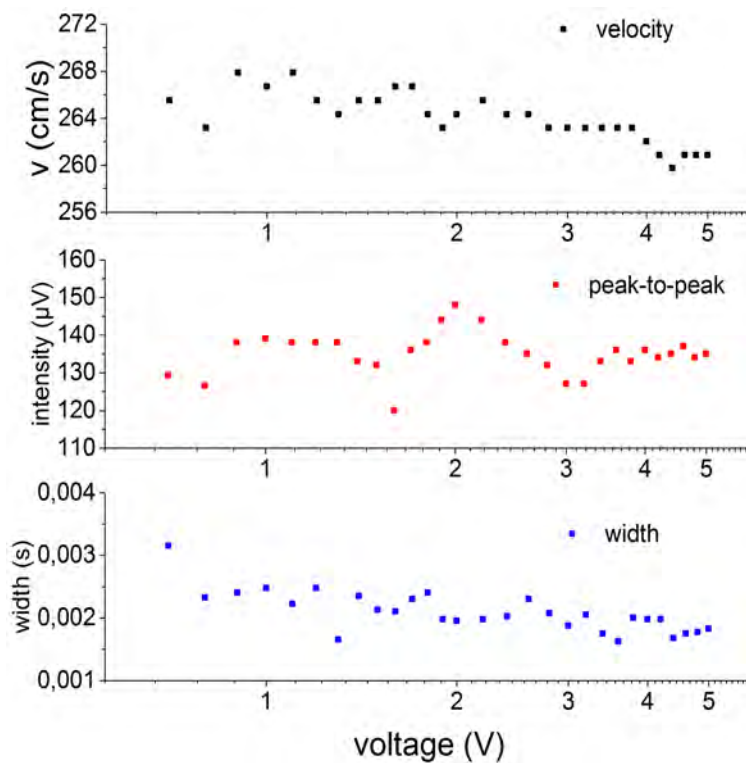


Figure 3.12: Behaviour of width, propagation velocity and intensity (peak-to-peak) 19.1.01 for the second peak orthodromic

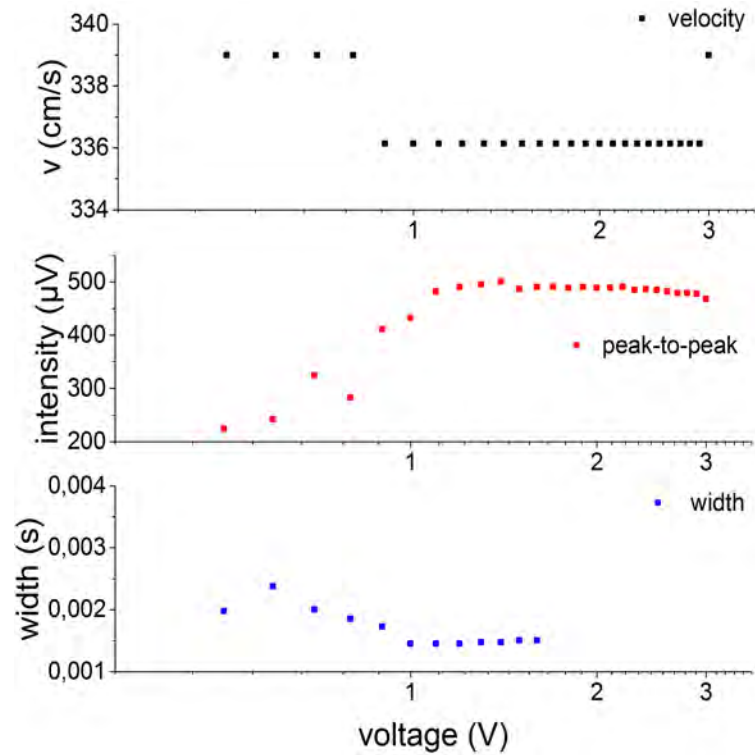


Figure 3.13: Behaviour of width, propagation velocity and intensity (peak-to-peak) 14.1.05 the first peak orthodromic

Figure 3.10 and 3.11 undergird a threshold of the stimulation voltage of 2V. The values for velocity, as well for intensity and width shown in figures 3.12 and 3.13, are not reliable for stimulation voltages below 2V, because the relative positions of the peaks can be changed by new occurring peaks, i.e. new stimulated neurons.

Note that intensity and width are difficult to determine due to the overlapping of peaks and we will not use these parameters for calculations or inferences. However in well defined, isolated peaks it could be possible to determine these parameters.

The propagation velocity was now normalized by the value of the velocity at stimulation with 2 V, in order to compare the full set of data. In the following paragraph (figures 3.14 -3.17) we will show the conduction velocities, corresponding to the first and second peaks, in orthodromic and antidromic direction for our two categories of legs. In these figures we only show a selection of data as an example. As mentioned measurements where new peaks occur above the threshold voltage were not regarded, e.g. 14.1.01.

The same procedure was used to analyse the velocities correlating to the second peaks.

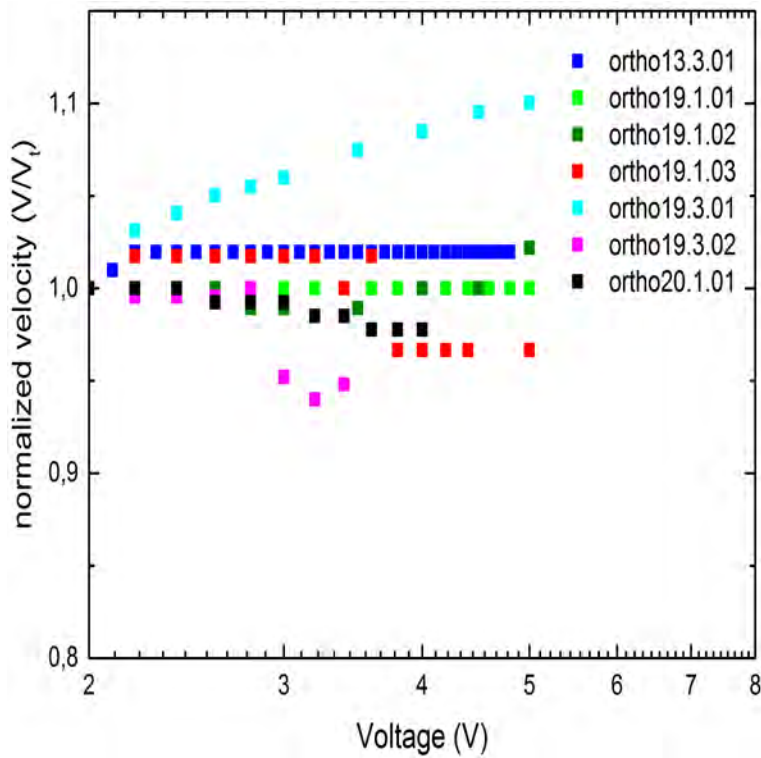


Figure 3.14: In the threshold (V_t) normalized conduction velocities of first peaks in orthodromic direction in leg category "Claw" as function of the stimulation voltage.

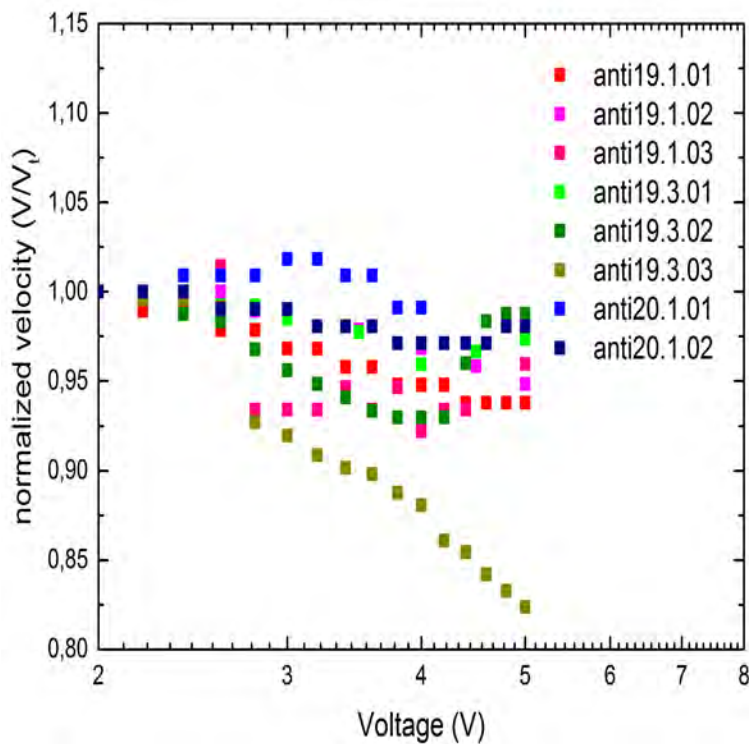


Figure 3.15: In the threshold (V_t) normalized conduction velocities of first peaks in antidromic direction in leg category "Claw", as a function of the stimulation voltage.

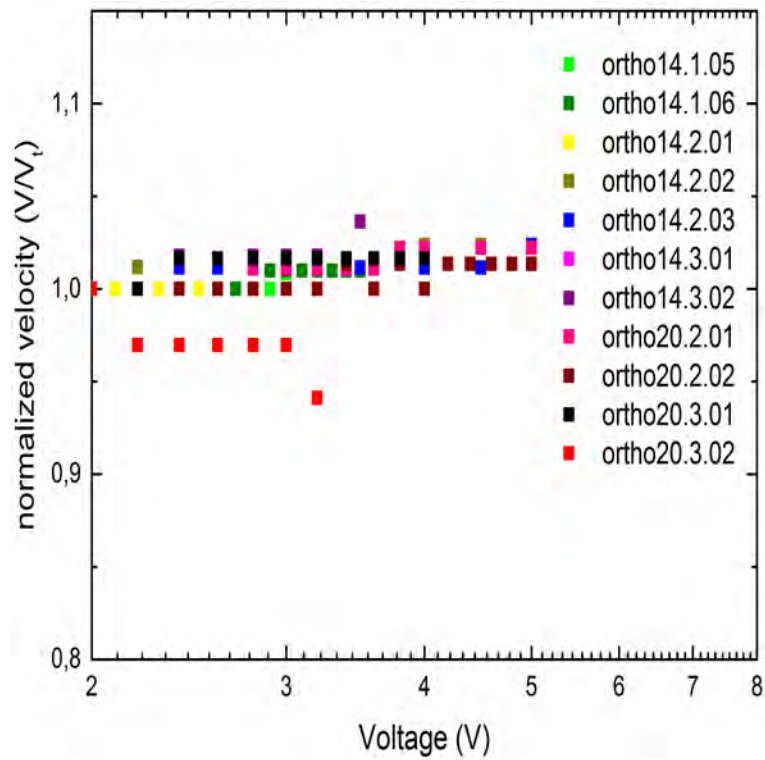


Figure 3.16: In the treshold (V_t) normalized conduction velocities of first peaks in orthodromic direction in leg category "NoClaw", as a function of the stimulation voltage.

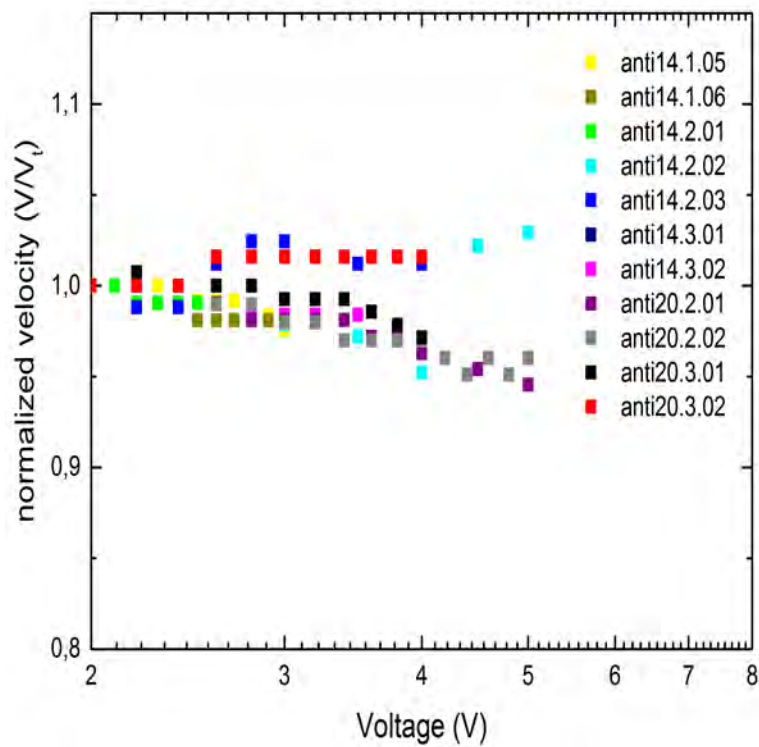


Figure 3.17: In the treshold (V_t) normalized conduction velocities of first peaks in antidromic direction in leg category "NoClaw", as a function of the stimulation voltage.

In order to summarize our results we averaged the values of the normalized velocities in orthodromic and antidromic direction for each stimulation voltage and the two categories of legs, respectively. The results were fitted with a linear polynome in order to compare the general trends of each respresented peak. In figures 3.18 - 3.21 we show the averaged velocities in antidromic and orthodromic direction for the first and second peaks of the legs with ("Claw") and without claw ("NoClaw").

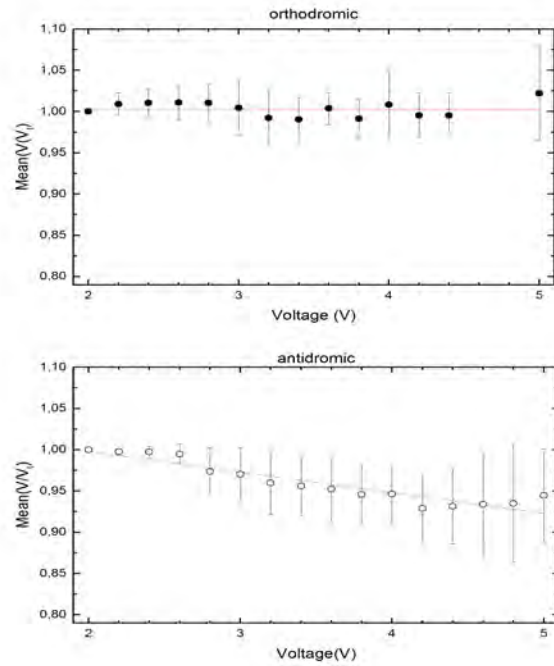


Figure 3.18: Normalized and averaged conduction velocities corresponding to the **first** peaks in orthodromic and antidromic direction for legs of "Claw". V_t is the treshhold voltage used for the normalization. Red line shows the linear fit and error bars the standard deviation of the averaged values.

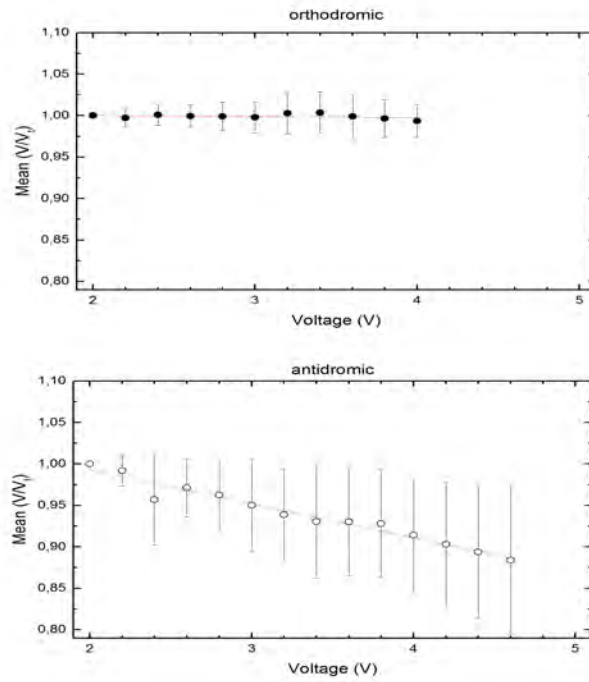


Figure 3.19: Normalized and averaged conduction velocities corresponding to the **second** peaks in orthodromic and antidromic direction for legs of "Claw". V_t is the threshold voltage used for the normalization. Red line shows the linear fit and error bars the standard deviation of the averaged values.

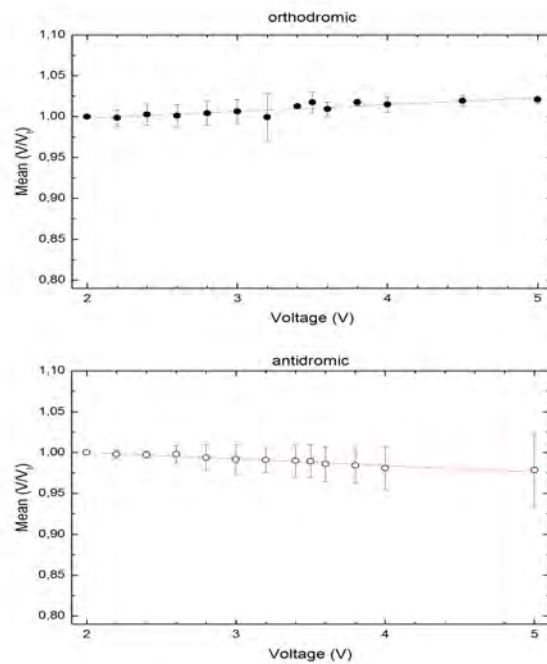


Figure 3.20: Normalized and averaged conduction velocities corresponding to the **first** peaks in orthodromic and antidromic direction for legs of "NoClaw". V_t is the threshold voltage used for the normalization. Red line shows the linear fit and error bars the standard deviation of the averaged values.

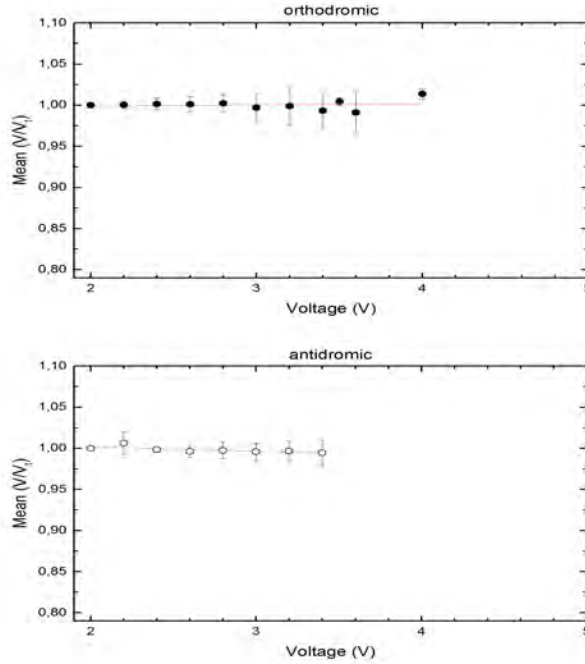


Figure 3.21: Normalized and averaged conduction velocities corresponding to the **second** peaks in orthodromic and antidromic direction for legs of "NoClaw". V_t is the threshold voltage used for the normalization. Red line shows the linear fit and error bars the standard deviation of the averaged values.

From the figures it is evident, that the propagation in the first two legs ("Claw") is asymmetrical as function of the stimulation voltage for the first and second peak, while in the third and fourth walking legs ("NoClaw") the propagation is almost perfectly symmetrical. In the following table, the slopes from the first two peaks for orthodromically and antidromically propagation is shown, for the two categories ("Claw", "NoClaw"), respectively.

Table 3.1: Slopes from figures 3.18 to 3.21 to comparison.

	"Claw"		"NoClaw"	
	First peak	Second peak	First peak	Second peak
orthodromic	0	-0,001	0,008	0,001
antidromic	-0,025	-0,041	-0,008	-0,005

It is important to note that the large giant axon ($diameter \leq 100\mu m$) are only present in the first and second walking leg. Controlling the claw they are absent in the third and fourth leg. Additionally it is expected that the axonal diameter is more uniform in the third and fourth legs, due to their smaller diameter. The differences in propagation velocity could be related with the changes in axonal diameter for the giant axons. The diameter gets larger close to the body or rather close to the soma, while it decreases in the bodies periphery, the claws. To point out: The axons diameter decreases with distance in the orthodromic direction and increases with distance in the antidromic direction. The stimulation voltage represents the energy necessary to depolarize a precise membrane area in the sensory bundle. The decay in propagation velocity in antidromic direction could be due to an increasing membrane area (increasing diameter) and a constant energy - or rather a decrease in the energy per unit of membrane area, expressed in the decreased velocity.

According to this idea the propagation velocity should increase in orthodromic direction, if the diameter decreases. It is plausible to assume, that the diameter change in antidromic direc-

tion is bigger than in orthodromic direction. The antidromically propagating AP is travelling in direction of the soma, which has a significantly larger diameter than the axon, while the orthodromically propagating AP stays in the axon, so that the changes in diameter are not significant. Additionally the result indicates that the higher the energy supply the membrane (higher stimulation voltage) the higher is the decrease in antidromically conduction velocity. Note that the assumption, that the diameter of the giant axons present in third and fourth walking legs is plausible, because the error bars of those preparations are noticeable smaller than those for the first and second walking legs. This indicates, that anatomically the neurons are more uniform between different animals for the third and fourth walking legs. The large error bars present on the first and second walking legs, are an indication of large polydispersity in the axons between different animals. It is also plausible, that small giant axons could have an asymmetrical AP propagation. However, the extension of this asymmetry is in any case lower than in the case of first and second walking legs. It will be interesting in future to investigate in more details the large bundles of the third and fourth legs as well as the medium and small bundles present in all walking legs, in order to examine possible asymmetries in bidirectional AP propagation.

Chapter 4

Conclusion

We investigated the effect of changing stimulation voltage on the bidirectional propagation of action potentials in the giant axons of lobster walking legs. The threshold stimulation voltage to generate action potentials propagating bidirectionally was found to be $\leq 2V$ for all nerve preparations. The threshold was approximately the same for orthodromic and antidromic propagating signals. The propagation velocity shows an asymmetric behaviour in bundles from legs with claw. The antidromic propagation velocity decreases with increasing stimulation voltage, probably due to the increase axon diameter in direction of the soma. The orthodromic propagation stays constant with increasing stimulation voltage. In the legs without claws the action potential propagation was found to propagate nearly symmetrical, i.e. antidromic and orthodromic propagation velocities didn't change with increasing stimulation voltage. Because axonal membrane-area changes in the large giant axon in first and second walking legs are more significant as in third and fourth walking legs, it is suggested that changes in surface area affect the propagation velocity of an action potential. With larger surface area the energy per area unit decreases. This decrease in energy per area unit is expressed in a decay of the conduction velocity.

Furthermore the propagation in antidromic direction shows an analogy (a decrease in energy per unit) with the backpropagation in neurons as reported by Stuart et al., that shows a decay in intensity of the backpropagating action potential with the distance from the soma.[14].

Appendix A

Appendix

Stimulation Voltage Measurement	2V	2,2V	2,4V	2,6V	2,8V	3V	3,2V	3,4V	3,6V	3,8V	4V	4,2V	4,4V	4,6V	4,8V	5V
13.3.01	1	1,0198	1,0198	1,0198	1,0198	1,0198	1,0198	1,0198	1,0198	1,0198	1,0198	1,0198	1,0198	1,0198	1,0198	
19.1.01	1	1	1	1	1	1	1	1	1	1	1	1	1	1	1	1
19.1.02	1	1	1	1	0,98936	0,98936	--	--	--	--	1	--	--	--	--	1,02198
19.1.03	1	1,01754	1,01754	1,01754	1,01754	1,01754	1,01754	1	1,01754	0,96667	0,96667	0,96667	0,96667	0,96667	0,96667	0,96667
19.3.01	1	1,03139	1,04072	1,05023	1,05505	1,05991	--	--	--	--	1,08491	--	--	--	--	1,10048
19.3.02	1	0,99545	0,99545	0,99545	1	0,95217	0,93991	0,94805								
20.1.01	1	1	1	0,99248	0,99248	0,99248	0,98507	0,98507	0,97778	0,97778	0,97778					

Figure A.1: Normalized and averaged conduction velocities corresponding to the **first** peaks in orthodromic direction for legs of "Claw".

Stimulation Voltage	2V	2,2V	2,4V	2,6V	2,8V	3V	3,2V	3,4V	3,6V	3,8V	4V	4,2V	4,4V	4,6V	4,8V	5V
Measurement																
19.1.01	1	0,98913	0,98913	0,97849	0,97849	0,96809	0,96809	0,95789	0,95789	0,94792	0,94792	0,94792	0,93814	0,93814	0,93814	0,93814
19.1.02	1	1	1	1	0,98925	0,98925	--	--	--	--	0,96842	--	--	--	--	0,94845
19.1.03	1	1	1	1,01429	0,93421	0,93421	0,93421	0,94667	0,93421	0,94667	0,92208	0,93421	0,93421	--	--	0,95946
19.3.01	1	1	0,99615	0,99234	0,99234	0,98479	--	--	--	--	0,95926	--	--	--	--	0,97368
19.3.02	1	0,99583	0,9876	0,98354	0,96761	0,956	0,94841	0,94094	0,93359	0,92996	0,92996	0,92996	0,95984	0,98354	0,9876	0,9876
19.3.03	1	0,99565	0,99565	0,99134	0,92713	0,91968	0,90873	0,90157	0,89804	0,8876	0,88077	0,8609	0,85448	0,84191	0,83273	0,82374
20.1.01	1	1	1,00909	1,00909	1,00909	1,01835	1,01835	1,00909	1,00909	0,99107	0,99107					
20.1.02	1	1	1	0,9902	0,9902	0,9902	0,98058	0,98058	0,98058	0,97115	0,97115	0,97115	0,97115	0,97115	0,98058	0,98058

Figure A.2: Normalized and averaged conduction velocities corresponding to the **first** peaks in antidromic direction for legs of "Claw".

Stimulation Voltage	2 V	2,2 V	2,4 V	2,6 V	2,8 V	3 V	3,2 V	3,4 V	3,6 V	3,8 V	4 V
Measurement											
13.3.01	1	1,00746	1,02273	1,02273	1,03053	1,03053	1,03846	1,03846	1,03053	1,02273	1,02273
19.1.01	1	1	1	0,9918	0,9918	0,98374	0,98374	0,98374	0,98374	0,98374	0,98374
19.1.02	1	0,97727	0,98473	0,98473	0,98473	0,98473	--	--	--	--	0,98473
19.3.01	1	1,0035	1,0035	1,00702	1,00702	1,01056					
19.3.02	1	1,00714	1	0,99647	0,99296	0,98947	1	1,00356			
19.3.03	1	0,99145	--	--	--	--	--	--			
20.1.01	1	0,99412	0,99412	0,99412	0,9883	0,9883	0,9883	0,9883	0,98256	0,98256	0,98256

Figure A.3: Normalized and averaged conduction velocities corresponding to the **second** peaks in orthodromic direction for legs of "Claw".

Stimulation Voltage	2V	2,2V	2,4V	2,6V	2,8V	3V	3,2V	3,4V	3,6V	3,8V	4V	4,2V	4,4V	4,6V
Measurement														
13.3.01	1	1,0082	0,94615	0,92481	0,90441	0,87234	0,88489	0,86014	0,8662	0,8662	0,86014	0,84247	0,83108	0,8255
19.1.01	1	1,00442	1	1	0,99561	0,99561	0,99561	0,99561	0,99561	0,99561	0,99127	0,98696	0,98268	0,98696
19.1.03	1	0,98496	0,97037	0,96324	0,9562	0,94928	0,93571	0,93571	0,92908	0,92254	0,89116	0,87919	0,86755	0,83974
19.3.01	1	1	1	0,99669	0,9934	0,98366	--	--	--	--	--	--	--	--
19.3.03	1	0,96262	0,86798	--	--	--								

Figure A.4: Normalized and averaged conduction velocities corresponding to the **second** peaks in antidromic direction for legs of "Claw".

Stimulation Voltage Measurement	2 V	2,2 V	2,4 V	2,6 V	2,8 V	3 V	3,2 V	3,4 V	3,5 V	3,6 V	3,8 V	4 V	4,5 V	5 V
14.1.05	1	1	1	1	1	1,00847								
14.1.06	1	1	1	1	1	1,0099	1,0099	1,0099	1,0099	--	--	--		
14.2.01	1	1	1											
14.2.02	1	1,01176	1,01176	1,01176	1,01176	1,01176	--	--	1,01176	--	--	1,02381	1,02381	1,02381
14.2.03	1	1	1,01163	1,01163	1,01163	1,01163	--	--	1,01163	--	--	1,01163	1,01163	1,02353
14.3.01	1	1	1	--	--	--	--	--	--	--	--	--	--	--
14.3.02	1	1	1,01786	1	1,01786	1,01786	1,01786	--	1,03636	--	--	--		
20.2.01	1	1	1	1	1,01099	1,01099	1,01099	1,01099	--	1,01099	1,02222	1,02222	1,02222	1,02222
20.2.02	1	1	1	1	1	1	1	1,01351	--	1	1,01351	1	--	1,01351
20.3.01	1	1	1,01639	1,01639	1,01639	1,01639	1,01639	1,01639	--	1,01639	1,01639	1,01639		
20.3.02	1	0,9697	0,9697	0,9697	0,9697	0,9697	0,94118							

Figure A.5: Normalized and averaged conduction velocities corresponding to the **first** peaks in orthodromic direction for legs of "NoClaw".

Stimulation Voltage	2 V	2,2 V	2,4 V	2,6 V	2,8 V	3 V	3,2 V	3,4 V	3,5 V	3,6 V	3,8 V	4 V	5 V
Measurement													
14.1.05	1	1	1	0,99174	0,98361	0,97561							
14.1.06	1	0,99038	0,99038	0,98095	0,98095								
14.2.01	1	0,99057	0,99057										
14.2.02	1	1	1	1	0,98592	0,97902	--	--	0,97222	--	--	0,95238	1,02941
14.2.03	1	0,98824	0,98824	1,01205	1,02439	1,02439	--	--	1,01205	--	--	1,01205	--
14.3.01	1	1	1										
14.3.02	1	1	1	1	0,98413	0,98413	0,98413	--	0,98413				
20.2.01	1	1	1	0,99048	0,98113	0,98113	0,98113	0,98113	--	0,97196	0,97196	0,96296	0,94545
20.2.02	1	1	1	0,9898	0,9898	0,9798	0,9798	0,97	--	0,97	0,97	0,97	0,9604
20.3.01	1	1,00735	1	1	1	0,99275	0,99275	0,99275	--	0,98561	0,97857	0,97163	
20.3.02	1	1	1	1,01613	1,01613	1,01613	1,01613	1,01613	--	1,01613	1,01613	1,01613	

Figure A.6: Normalized and averaged conduction velocities corresponding to the **first** peaks in antidromic direction for legs of "NoClaw".

Stimulation Voltage	2 V	2,2 V	2,4 V	2,6 V	2,8 V	3 V	3,2 V	3,4 V	3,5 V	3,6 V	4 V
Measurement											
14.1.01	1	1	1	1	1	1	0,99254	0,99254	--	1	1,00758
14.1.05	1	0,99351	0,9871	0,9871	0,98077	0,97452					
14.1.06	1	1	1,00714	1,00714	1,00714	1,00714	1,00714	1,00714	1		
14.2.01	1	1	1	1	1,00645	1					
14.2.02	1	1	1	1	1,0087	1	--	--	1,0087	--	1,0087
14.2.03	1	1	1,00862	1,00862	1,00862	1,00862	--	--	1,00862	--	1,01739
14.3.02	1	1,01087	1,01087	1,01087	1,01087	1,01087	1,02198	--	1		
20.3.01	1	1	1	1,01042	1,01042	1,01042	1,01042	1,01042	--	1,01042	1,02105
20.3.02	1	1	1	0,98718	0,98718	0,9625	0,9625	0,9625	--	0,9625	

Figure A.7: Normalized and averaged conduction velocities corresponding to the **second** peaks in orthodromic direction for legs of "NoClaw".

Stimulation Voltage	2 V	2,2 V	2,4 V	2,6 V	2,8 V	3 V	3,2 V	3,4 V
Measurement								
14.1.05	1	1	1	1	1	0,99371		
14.1.06	1	1	0,99265	0,9854	0,9854	0,9854	0,9854	0,97826
14.2.03	1	1,03175	1					
20.3.01	1	1	1	1	0,99468	0,99468	0,99468	0,99468
20.3.01	1	1	1	1	1,0099	1,0099	1,0099	1,0099

Figure A.8: Normalized and averaged conduction velocities corresponding to the **second** peaks in antidromic direction for legs of "NoClaw".

Bibliography

- [1] R. Appali, S. Petersen, and U. van Rienen. A comparison of Hodgkin-Huxley and soliton neural theories. *Advances in Radio Science*, 8:75–79, Sept. 2010.
- [2] T. Branco and M. Häusser. The selfish spike: local and global resets of dendritic excitability. *Neuron*, 61(6):815–7, Mar. 2009.
- [3] A. J. Darin De Lorenzo, M. Brzin, and W. D. Dettbarn. Fine structure and organization of nerve fibers and giant axons in *Homarus americanus*. *Journal of ultrastructure research*, 24(5):367–84, Sept. 1968.
- [4] DericBownds. <http://dericbownds.net/bom99/Ch02/Ch02.html> March 27th, 2014 1 pm.
- [5] A. J. Foust and D. M. Rector. Optically teasing apart neural swelling and depolarization. *Neuroscience*, 145(3):887–99, Mar. 2007.
- [6] D. K. Hartline and D. R. Colman. Rapid conduction and the evolution of giant axons and myelinated fibers. *Current biology : CB*, 17(1):R29–35, Jan. 2007.
- [7] T. Heimburg and A. D. Jackson. On soliton propagation in biomembranes and nerves. *Proceedings of the National Academy of Sciences of the United States of America*, 102(28):9790–5, July 2005.
- [8] A. L. Hodgkin and A. F. Huxley. A quantitative description of membrane current and its application to conduction and excitation in nerve. *The Journal of physiology*, 117(4):500–44, Aug. 1952.
- [9] E. R. Kandel. *Principle of neural Science*. 2012.
- [10] T. Matheson. Invertebrate Nervous Systems. pages 1–6, 2002.
- [11] J. R. Morgan and O. Bloom. *Cells of the nervous system*. 2005.
- [12] D. Pinault. Backpropagation of action potentials generated at ectopic axonal loci: hypothesis that axon terminals integrate local environmental signals. *Brain research. Brain research reviews*, 21(1):42–92, July 1995.
- [13] PowerLab. http://cdn.adinstruments.com/adi-web/manuals/PowerLab_Teaching_15_26_OG.pdf March 27th, 2014 1 pm.
- [14] G. Stuart, N. Spruston, B. Sakmann, and M. Häusser. Action potential initiation and backpropagation in neurons of the mammalian CNS. *Trends in neurosciences*, 20(3):125–31, Mar. 1997.
- [15] G. M. Villegas and F. Sánchez. Periaxonal ensheathment of lobster giant nerve fibres as revealed by freeze-fracture and lanthanum penetration. *Journal of neurocytology*, 20(6):504–17, June 1991.
- [16] J. Waters, A. Schaefer, and B. Sakmann. Backpropagating action potentials in neurones: measurement, mechanisms and potential functions. *Progress in biophysics and molecular biology*, 87(1):145–70, Jan. 2005.